



Optimal parameter(s) for the synthesis of nitrogen-vacancy (NV) centres in polycrystalline diamonds at low pressure

Hammed A. Ejalonibu¹ · Gordon E. Sarty^{1,2} · Michael P. Bradley²

Received: 21 February 2019 / Accepted: 19 April 2019 / Published online: 25 April 2019
© Springer Science+Business Media, LLC, part of Springer Nature 2019

Abstract

Nitrogen-vacancy (NV) centres in diamonds are emerging quantum materials having applications in quantum computing and magnetic field sensing. The ability to synthesize polycrystalline diamond films from chemical vapour deposition technique offers a possibility to grow cheap diamonds with NV centres over large areas. Till date, extensive studies have not been carried out to understand the influence of nitrogen flow rate on the formation of NV centres in polycrystalline diamonds. In this study, we investigate the effect of nitrogen flow rate on the morphology, optical, and electrical properties of polycrystalline diamonds deposited at low pressure. Several samples were prepared in different nitrogen flow regimes using the microwave plasma chemical vapour deposition (MPCVD) technique. The films were characterized using Raman spectroscopy and scanning electron microscopy (SEM). The I–V characteristics of the samples were measured using a point contact method at room temperature. Results obtained showed the formation of both neutral and negatively charged NV centres at an optimum nitrogen flow rate of 10 sccm. An increase in nitrogen flow rate led to a decrease in the electrical resistivity of the films. Furthermore, nitrogen flow rates greater than 20 sccm results to a decrease in the reflectance spectra of samples and a depreciation in the crystalline quality of films. This study is important in benchmarking an optimal parameter space for the growth of nitrogen doped polycrystalline diamonds suitable for sensing applications.

1 Introduction

The intrinsic properties of diamond such as its extreme hardness, high wear resistance [1–3], thermal stability [4–8], optical and electrical properties [9–12] renders it a material of interest for numerous technological applications. Diamond finds application in biomedical implantation due to its hardness and high wear resistance [13]. Its thermal stability and outstanding electrical properties have been utilized for high power electronic devices [14–16]. Furthermore, its optical properties are harnessed in nanoscale magnetometry [17, 18], quantum information, quantum metrology, thermometry, dosimetry, and biosensing [19–21].

The incorporation of dopants/impurities like lithium, boron, silicon, and nitrogen during the chemical vapour deposition (CVD) process of diamond can profoundly alter

its intrinsic properties [22]. For instance, when impurities are trapped in defects formed during the CVD growth of diamonds, optical centres can be formed. Optical centres, commonly known as colour centres are solid-state qubits with the potential to be hosted in diamond. They are responsible for the numerous colours of diamonds. Examples of optical centres in diamond includes nitrogen-vacancy (NV) centres, silicon-vacancy (SiV) centres, and germanium-vacancy (GeV) centres. These centres have a wide range of application in physics, material science, and biotechnology [23]. An ensemble of NV centre found in diamonds can be used for sensing and imaging weak magnetic fields. A good coherence property of the spin sensor will enable its use in developing low-field magnetic resonance imaging (MRI) detectors. Also, the single NV centre in diamond are recently employed for rudimentary magnetic resonance spectroscopy (NMR) of nanoscale samples and proteins [24], thus allowing the properties of these samples to be studied at the nanoscale level. All these applications will be referred to as “sensing applications” in later paragraphs.

In the last few decades, research attention has been directed towards the study of the incorporation of impurities in the CVD growth process of single and polycrystalline

✉ Hammed A. Ejalonibu
hammed.ejalonibu@usask.ca

¹ Division of Biomedical Engineering, University of Saskatchewan, Saskatoon, SK, Canada

² Department of Physics and Engineering Physics, University of Saskatchewan, Saskatoon, SK, Canada

diamonds. Experimental studies [25, 26] have shown that the incorporation of the right amount of nitrogen impurities in diamonds will lead to an improvement in its dosimetric properties; for use as a radiation detector. In addition, an optimized nitrogen incorporation in single crystal diamond will result in the creation of high-density NV centres. Moreover, there is a need to study the effect of other impurities on the CVD growth of diamond. To address this, Yap et al. [27] successfully showed that the incorporation of boron impurities in homoepitaxially grown CVD diamond does not result in the formation of nitrogen-related optical features. The observed feature may be due to the competition of boron impurities for vacancies, thereby leaving a small number of vacancies for nitrogen [28].

In general, impurities can be incorporated in several bonding configurations [25]. For example, the incorporation of nitrogen impurities in polycrystalline diamonds might lead to the formation of single substitutional nitrogen, vacancies with complexes, lattice defects or even nitrogen located at grain boundaries. Each bonding configuration is formed under different conditions, therefore, precisely controlled growth parameters (most especially, the nitrogen flow rate) are required. There has been much progress in the study of nitrogen incorporation in the CVD of diamonds. Despite this progress, the influence of nitrogen flow rates on the formation of NV centres in polycrystalline diamonds at low pressure has not been studied to date. In this study, we report the effect of nitrogen flow rates on the formation of useful NV centres in polycrystalline diamonds deposited at low pressure (4 kPa). In particular, the effect of nitrogen incorporation was investigated under different flow regimes. The novelty of the research presented here is to determine an optimal and reproducible nitrogen flow rate parameter for the synthesis of useful NV centres in polycrystalline diamonds. The study is essential because it provides information for the growth of polycrystalline diamonds suitable for sensing applications.

Here, some experiments have been carried out in a microwave plasma enhanced chemical vapour deposition (MPCVD) chamber using a mixture of $H_2/CH_4/N_2$ as the feed gases in order to systematically investigate the effect of surface impurities on the morphology, optical, and electrical properties of polycrystalline CVD diamonds deposited at low pressure. The work here differs from other work as follows. Earlier work on the incorporation of impurities in Refs. [27, 29] introduced impurities from the beginning in the gas phase. Here, the effect of surface impurities introduced for a period of time close to the end of the experiment was examined. The motivation behind this approach arose from the need to locate optical centres needed for sensing applications within a few nanometers of the surface. The effect of nitrogen was investigated under three flow regimes; low nitrogen addition (0 sccm), medium nitrogen addition (1–4

sccm), and high nitrogen addition (10–40 sccm). Furthermore, we note that past approaches introduced impurities while working at moderate pressure (9.3–27 kPa). In contrast, the characteristics of these films under relatively low working pressure (4 kPa) were examined here. The results obtained are important in benchmarking optimal parameters for the growth of nitrogen doped polycrystalline diamonds that are suitable for sensing applications.

2 Experimental details

2.1 Diamond film preparation

Polycrystalline diamond (PCD) films were deposited on a $3 \times 3 \times 0.5 \text{ mm}^3$ P-type boron doped silicon substrate of resistivity $5 \Omega \text{ cm}$ (Silicon Material Inc.) in a 2.45 GHz MPCVD reactor (Plasmionique Inc.). The silicon substrate has a $\langle 100 \rangle$ orientation. Prior to growth, the silicon substrates were nucleated by treating the surface with a mixture of diamond powder and ethyl-alcohol in an ultrasonic bath for 30 min. A stainless steel disk was used as the substrate holder in the deposition chamber. The manufacturer's details on the construction of the CVD reactor used can be found in Ref. [30].

Before deposition, the chamber was evacuated to a baseline pressure of $4.9 \times 10^{-3} \text{ Pa}$ via a turbo molecular pump. At this pressure, some nitrogen gas (less than 1%) is trapped in the chamber [25]. Operating at this baseline pressure makes it possible to define low nitrogen flow rates without the intentional addition of nitrogen. Gas mixtures consisting of $H_2/CH_4/N_2$ were varied in the chamber (see Table 1 for details). Diamond deposition was carried out at 800 W microwave power and 4 kPa pressure. The duration of each deposition run was 14 h. For samples in the medium and high nitrogen flow regimes, nitrogen gas was introduced for a period of time close to the end of the experiment, see details in Table 1.

2.2 Diamond film characterization

The microstructure and photoluminescence (PL) of the samples were studied using Raman Spectroscopy (Renishaw InVia). Raman spectroscopy can be used to detect structural defects and stress distribution in materials [31, 32]. All Raman and PL spectra were fitted with a sum of Lorentz functions (using the WiRE Raman Renishaw software) to identify peaks of interest. The Raman signals were collected using a $\times 50$ objective focusing the beam on a $20 \mu\text{m}$ diameter spot. The spectra collected at different spots on the samples were averaged. The PL emissions were collected using a $\times 20$ objective focusing the beam on a $50 \mu\text{m}$ diameter spot. For each spectra acquisition, a laser power of 0.010 W with

Table 1 Growth parameters for the deposition of diamond films on silicon substrate at 4 kPa pressure, 800 W microwave power, and deposition temperature of 700 °C

Group	Sample	H ₂ -CH ₄ -N ₂ flow (sccm)	Growth time + Doping time (hrs)
1	S1	100–1–0	14 + 0
	S5	100–1–1.5	13 + 1
	S9	100–1–10	13 + 1
2	S2	200–1–0	14 + 0
	S6	200–1–2	12 + 2
	S10	200–1–20	12 + 2
3	S3	300–0.75–0	14 + 0
	S7	300–0.75–3	13 + 3
	S11	300–0.75–30	11 + 3
4	S4	400–0.5–0	14 + 0
	S8	400–0.5–4	10 + 4
	S12	400–0.5–40	10 + 4

Parameters include doping time (in hours), hydrogen, methane, and nitrogen flow rates. All volumetric flow rates are in standard cubic centimeters per minute (sccm)

an exposure time of 10 s was used. The reflectance spectra of the films were collected using a spectroscopic reflectometer (USB-650 Red Tide UV–Vis).

Field Emission Scanning Electron Microscope (FE-SEM, Hitachi SU8000) was used to characterize the surface morphology of the samples. Electron micrographs were taken using an acceleration voltage of 3 KV and $\times 15$ magnification. Meanwhile, the electrical properties of the films were determined by measuring the current–voltage (I–V) characteristics using a point contact method at room temperature. For the I–V measurement set-up, a copper probe was used to form point contact with the film while the second copper probe was used to connect the back of the wafer to obtain an ohmic contact. In the results and discussion section that follows, samples were compared in groups; samples grown with the same hydrogen and methane concentration while varying the nitrogen flow rate. Here, 0 sccm, 1.5–4 sccm, and 10–40 sccm represent the low, medium and high nitrogen flow rate doping regimes respectively.

3 Results

3.1 Physical appearance and Raman spectra of films

Table 2 summarizes the data obtained from micro-Raman analysis and visual inspection of samples. The full width half maximum (FWHM), centre of the diamond peak, and colour of films are reported. From the table, it is evident that the colour of deposited diamond changes depending

Table 2 Characteristics of the deposited samples: full width at half maximum (FWHM) of diamond peaks and center of diamond peaks were obtained from the Raman spectra

Group	Sample	FWHM (D) (cm ⁻¹)	Center of Diamond peak (cm ⁻¹)	Color
1	S1	8.232	1331.2	Grey
	S5	7.695	1331.7	Lustrous grey
	S9	7.792	1332.0	Lustrous grey
2	S2	10.989	1331.3	Grey
	S6	11.268	1331.9	Lustrous grey
	S10	8.875	1331.9	Lustrous grey
3	S3	8.201	1332.0	Grey
	S7	13.320	1331.2	Grey
	S11	14.662	1332.5	Black
4	S4	8.586	1331.5	Grey
	S8	8.752	1331.4	Dark grey
	S12	15.463	1333.8	Black

Colour of deposited diamonds changes depending on the amount of nitrogen impurities in samples

on the amount of nitrogen impurities in the sample. Polycrystalline CVD diamonds grown heteroepitaxially without the addition of nitrogen impurities appeared grey in colour. Those grown with nitrogen impurities show a range of colours depending on the concentration of nitrogen in the sample.

Figure 1a and b show the Raman spectra of films in group 1 and 2. The spectra of films were presented with no particular preference. In these samples, we observe silicon peaks around 519 cm⁻¹, diamond peaks around 1332 cm⁻¹, D-band around 1345 cm⁻¹, and G-band around 1500–1600 cm⁻¹ [33]. The presence of both G and D-band results from amorphous carbon (*sp*²) related content located in the grain boundaries [34]. As seen in Fig. 1c, films grown with medium nitrogen flow rate in group 1 and 2 (i.e. S5 and S6) show almost similar spectra. The presence of this feature indicates that it might be difficult to differentiate spectra of films with quasi-similar nitrogen and methane concentrations during CVD [25].

The FWHM of a peak obtained from Raman spectroscopy gives an indication of the structural distribution of a material. For example, a crystalline material will show narrower peaks when compared to amorphous materials. It can also indicate the amount of disorder or defect density incorporated into the material [35]. From Table 2, reported FWHM for diamond deposited on Silicon (100) substrate is in the range 7.8–15.5 cm⁻¹. The observed FWHM of the deposited films is in good agreement with reported values in [36]. In reference to Fig. 1d, it can be seen that films doped with high nitrogen flow rate (30–40 sccm) in group 3 and 4 have larger FWHM than their counterparts.

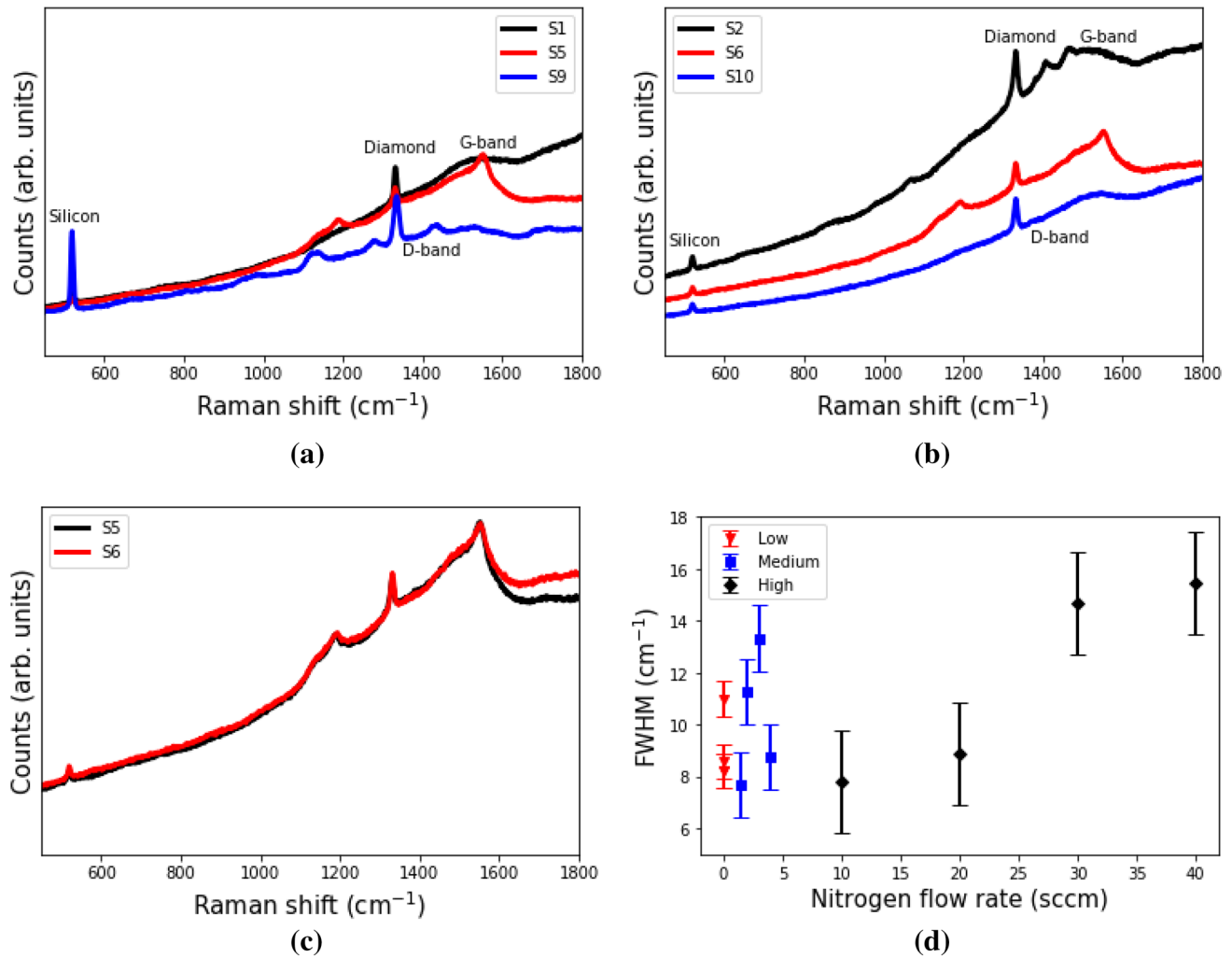


Fig. 1 Raman spectra of films **a** Raman spectra of films in group 1, **b** Raman spectra of films in group 2, **c** Raman spectra of films with medium nitrogen flow rate in group 1 and group 2, both films were

deposited with similar methane and nitrogen concentration **d** FWHM of diamond peaks against nitrogen flow rate, films with high flow rate (30–40 sccm) show larger FWHM

3.2 Morphology of films

Figure 2 shows the SEM micrographs of films. Distinct surface morphology is clearly exhibited as the nitrogen concentration is varied. Without the introduction of nitrogen dopants in the gas phase, the films consist of randomly oriented grains with rough surfaces. Samples doped with low and high nitrogen flow rates have particle sizes ranging from 1.3 to 2.5 ± 0.08 μm . The difference in grain sizes for these samples may be attributed to the different flow rates of hydrogen, methane, and nitrogen feed gas used. With the incorporation of medium (1.5–2 sccm) nitrogen flow rate in the gas phase mixture, surface morphology reveals dense nano-sized grains in the films. The grain size of the nanocrystalline films were calculated using the model reported by Cañado et al. [37] as shown in Eq. 1,

$$L_a(\text{nm}) = (2.4 \times 10^{-10}) \lambda_l^4 \left(\frac{I_{D_a}}{I_G} \right)^{-1} \quad (1)$$

where λ_l is the laser line wavelength (514.5 nm) used in the experiment; I_{D_a} and I_G are the integrated intensities of the diamond and graphite bands. Nano grained samples have grain size of 21 ± 0.46 nm.

To further validate results from Raman spectroscopy, the surface morphology of samples grown with medium nitrogen flow rates in group 1 and 2 (S5 and S6) were observed. These films have similar morphological features. A closer observation from the SEM micrographs revealed the presence of cracks in the sample S6 (see Fig. 2e) which might be due to stress and as a consequence increased the FWHM of this sample. With regards to the previous physical observation for highly doped diamonds, surface

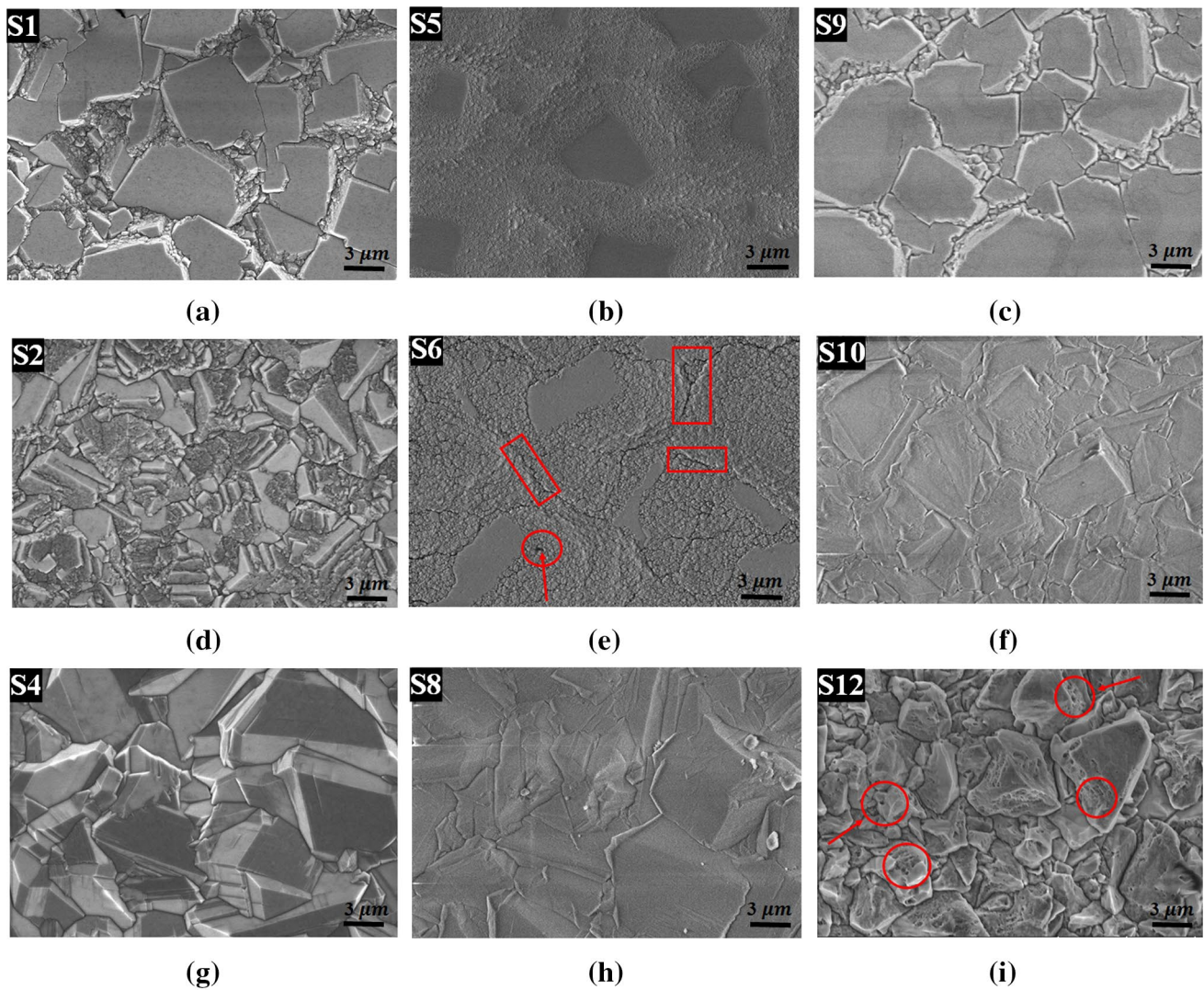


Fig. 2 Surface morphology of films, **a–c** surface morphology of samples in group 1, rough surfaces. Samples doped with low and high **d–f** surface morphology of samples in group 2, **g–i** surface morphology of samples in group 4

morphology of samples S12 (as in Fig. 2i) show heavily defective diamond grains with grains having several surface pores.

3.3 Photoluminescence (PL) and reflectance spectra of films

For the films to be used for sensing applications, the presence of optically active NV^- centers located close to the surface is important. To investigate the incorporation of surface optical centers, a room temperature photoluminescence (PL) measurement was performed. Figures 3, 4 show the PL spectra of films. The observed sharp distinguishable peaks in the spectra are at 515, 529, and 552 nm. The 515 nm lines are due to the Ar ion laser; the 529 nm

lines are due to the silicon substrate, and the 552 nm peaks are that of diamond [38, 39]. Broad peaks due to amorphous related elements are observed between 555 and 560 nm. Neutral optical centers peak (NV^0) occur around 575 nm, while negatively charged optical centres have peaks around 637 nm (NV^-) [26, 40, 41].

In summary, samples in group 1 (S5 and S6), a sample in group 2 (S10), and samples in group 4 (S8 and S12) show the presence of NV^0 . Only sample S9 in group 1 shows a tiny broad peak indicating the presence of NV^- . Shown in Fig. 4(b) is a normalized intensity bar graph of samples having nitrogen related optical features that can be harnessed for sensing. From Fig. 4b, sample S8 in group 4 has the greatest intensity of NV^0 as measured by PL spectroscopy, while S10 in group 2 has the lowest intensity.

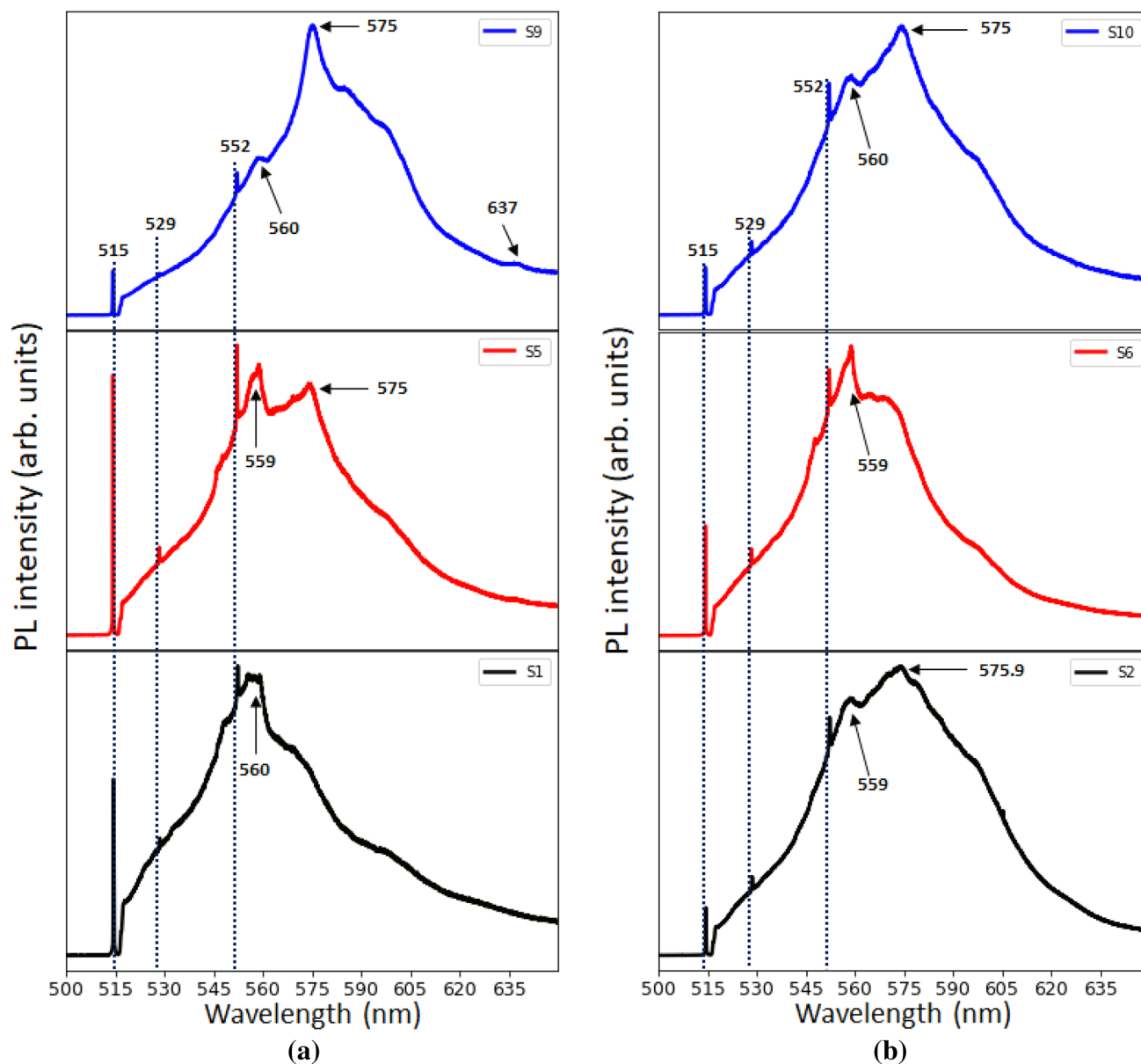


Fig. 3 Photoluminescence spectra of diamonds films **a** photoluminescence spectra of films in group 1, **b** photoluminescence spectra of films in group 2

In using this material for magnetic sensing applications, a reasonable photon collection efficiency should be achieved. NV centres suffer from a finite collection efficiency and light trapping due to total internal reflection and imperfections [42] in the host diamond. The imperfections reduce the contrast of optically detected magnetic resonance (ODMR) when the material is used as a magnetic field sensor. To further determine the effect of nitrogen flow rates on the expected contrast of the sensors, the relative reflectance of the deposited films were compared. Since the thickness of films play a role in the intensity

of collected light, the cross section of films were imaged to determine the thickness and shown in Fig. 5. For the growth parameters used, no considerable increase in film thickness was recorded after 12 h of growth even with the subsequent introduction of nitrogen gas, thus making it possible to compare samples in groups. The mean thickness of samples in group 1 and group 4 were found to be $11 \pm 0.1 \mu\text{m}$ and $2.5 \pm 0.07 \mu\text{m}$ respectively. Figure 6 shows the reflectance spectra of the deposited films. From the spectra obtained in Fig. 6a, we observe that introducing 1–10 sccm nitrogen impurities does not have any effect

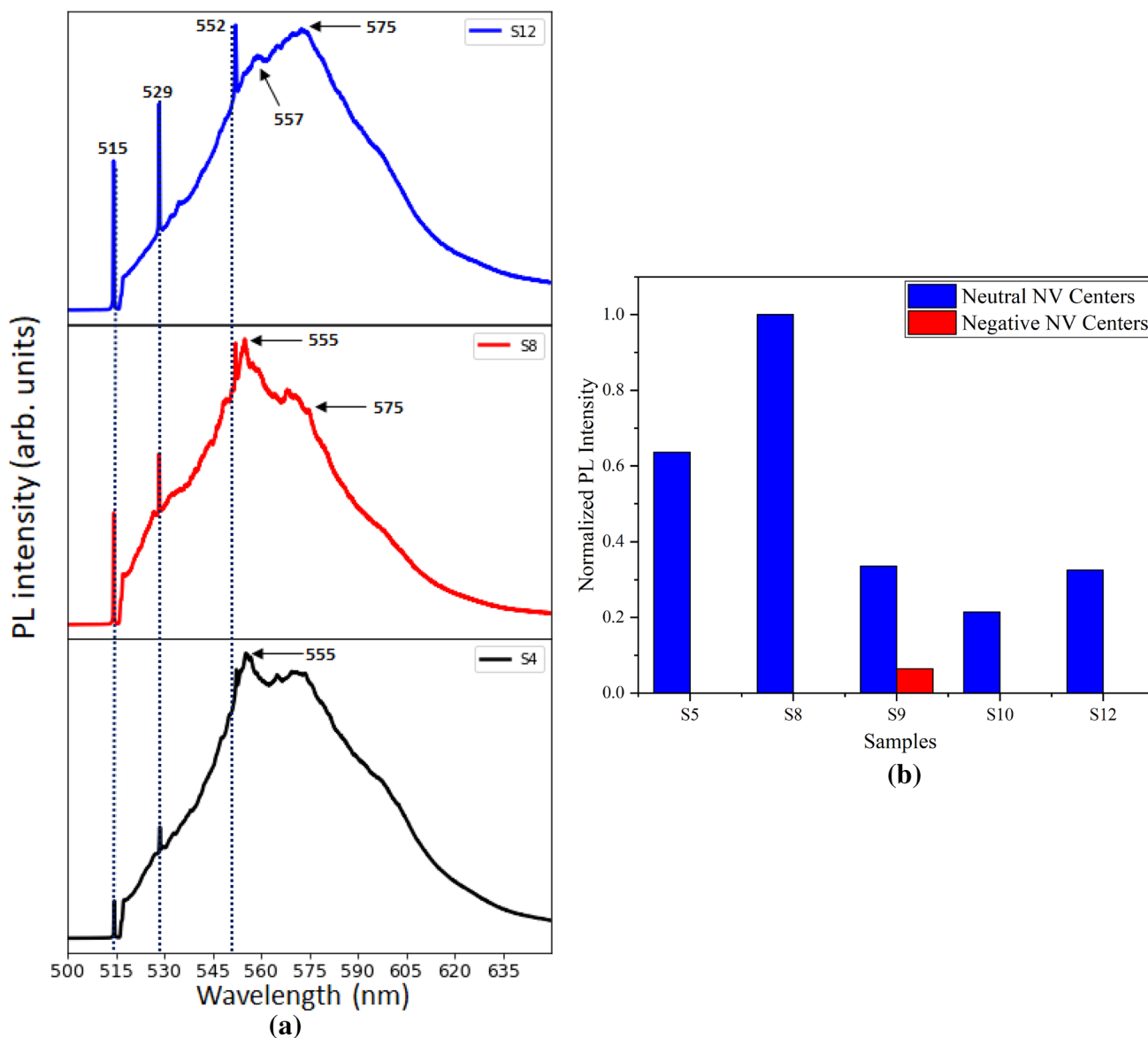


Fig. 4 Photoluminescence spectra of diamonds films **a** photoluminescence spectra of films in group 4, **b** Normalized PL intensity of NV⁻ and NV⁰ in diamond samples

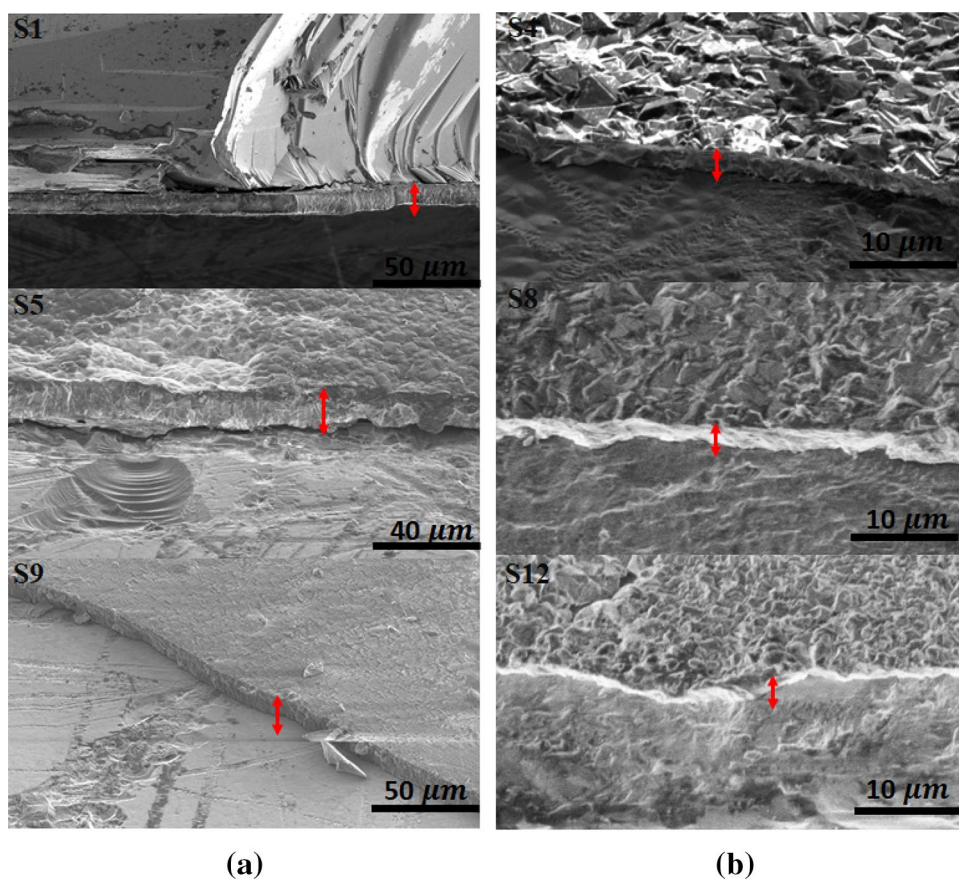
on the reflectance of the material. Outside this regime, the reflectance of the deposited films is seen to decrease with excess nitrogen impurity level in the material (as shown in Fig. 6b–d).

3.4 Electrical properties of films

A study of the I–V characteristics of the deposited films is presented here. The current density of the deposited films as a function of the anode voltages were compared. Shown in Fig. 7 is the *J* vs. *E* curves of samples in group 2 and 4. From these plots, the turn-on field and emission

current density can be obtained. The electrical resistivity of these samples were calculated by taking the inverse of the slope obtained from a power fit of $I = aV^b$ of the current density vs. voltage curves. See Table 3 for electrical resistivity of these films. From the table, one can conclude that there is a decrease in the surface electrical resistance upon doping with high nitrogen flow rate. Figure 8 shows the variation of surface resistivity of doped samples with the flow rate of nitrogen gas. From the plot, we report a decrease in the electrical resistivity as the nitrogen flow rate is increased.

Fig. 5 Cross-section SEM images of films **a** cross-section SEM images of samples in group 1, **b** cross-section SEM images of samples in group 4



4 Discussion

4.1 Physical appearance and Raman spectra of films

The grey and lustrous grey colour of the deposited diamonds results from the dispersions created by different planes of the grains in the film. Dark grey and black colourations seen in doped diamonds may be due to extended defects from hydrogen atom impurities, dislocation density, and impurities in the lattice [43]. Notably, the incorporation of a high flow rate of nitrogen with a nitrogen-carbon [N/C] ratio greater than 30 in the gas phase mixture leads to black coloured diamonds. Black coloured CVD diamonds are heavily defective with a large quantity of impurity and presence of graphitic grains [44]. The identical spectra of samples with medium nitrogen flow rates (S5 and S6) indicates that a 0.5 sccm difference in flow rate is insignificant to change the microstructure of films grown with similar methane concentration. The observation of the increase in the FWHM of Raman peak of highly doped samples indicates that the addition of a large amount of nitrogen impurity is detrimental to the crystalline quality of CVD diamonds. Using diamond peak at 1332 cm^{-1} as standard, the shift in the Raman wavenumber and the ratio of the intensity of diamond and amorphous

carbon peak (I_{Da}/I_G) is obtained and shown in Fig. 9. Negative Raman line shifts are due to compressive stresses in the films, while positive Raman line shifts are due to intrinsic stresses which are tensile in nature [35]. A high quantity of nitrogen impurity can introduce stress in the material [44]. This is confirmed by a shift in the diamond peak from ~ 1332 to 1334 cm^{-1} for highly doped samples (sample S12). For sensing applications, black coloured diamonds are undesirable due to the high concentration of amorphous carbon which quenches photoluminescence from the NV^- centres. A potential candidate for this application are experimental samples showing either grey or lustrous grey colourations with the presence of NV^- center.

4.2 Morphology of films

From the SEM micrograph results, insights into the formation of nitrogen related optical centres from a surface morphology perspective can be obtained. First, in small-sized nano-grain diamonds typical of diamonds doped with medium flow rates (1.5–2 sccm), it is believed nitrogen is being incorporated preferentially at grain boundaries [45] rather than in the grains. This is evident by results obtained

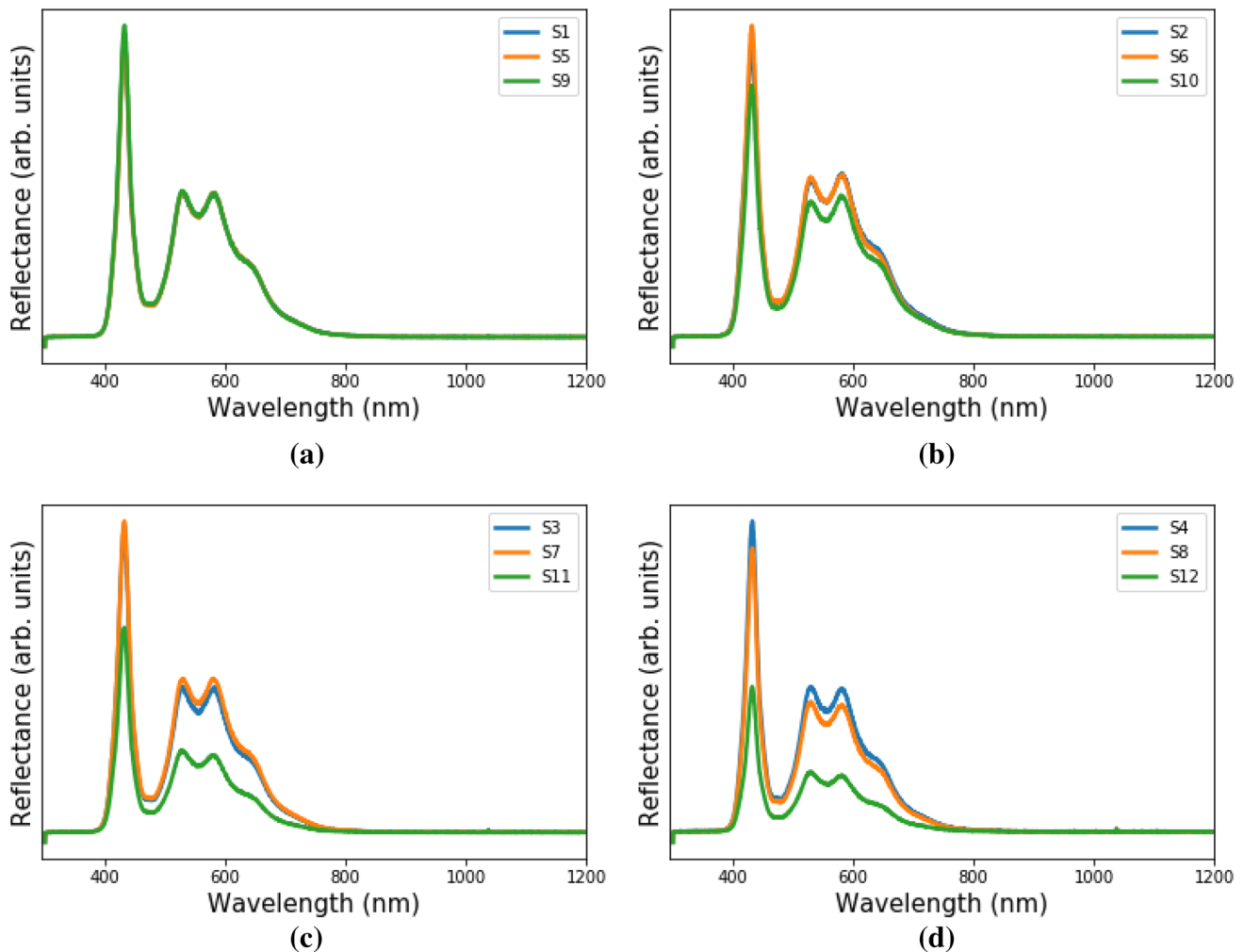


Fig. 6 Reflectance spectra of samples **a** reflectance spectra of samples in group 1, **b** reflectance spectra of samples in group 2, **c** reflectance spectra of samples in group 3, **d** reflectance spectra of samples in group 4

from tight-binding molecular dynamics simulations in [46]. It is also possible that vacancies are not easily incorporated in small-sized grain polycrystalline diamond with fine and continuous surface textures, therefore, bringing doped nitrogen to grain boundaries or even forming other complex configurations that are not of nitrogen vacancies. This may explain why there are no nitrogen related optical centres in sample S6 in group 2. Samples with little or no vacancies like sample S6 in group 2 may require further processing.

Vacancies can be created using a high energy electron irradiation beam [47]. Since nitrogen is present in grain boundaries or in other configurations, an additional annealing procedure will help migrate vacancies to form nitrogen-vacancies in the films. Apparently, nitrogen related optical centers can be formed via excessive doping

as shown by Ohno et al. [47] but at the expense of losing the crystalline quality of the diamond films. In addition, several authors including Schirhagl et al. [40] have reported a depreciation in the spin coherence properties of excessively doped films. Nevertheless, it is important to emphasize that sample S9 in group 1 maintained its crystalline structure despite the high nitrogen flow rate (10 sccm). This again points to the fact that sample S9 might be a suitable material for sensing applications.

4.3 Photoluminescence (PL) and reflectance spectra of films

Several publications [25–27, 29] have shown that when no extra effort is made to exclude residual nitrogen gas in the

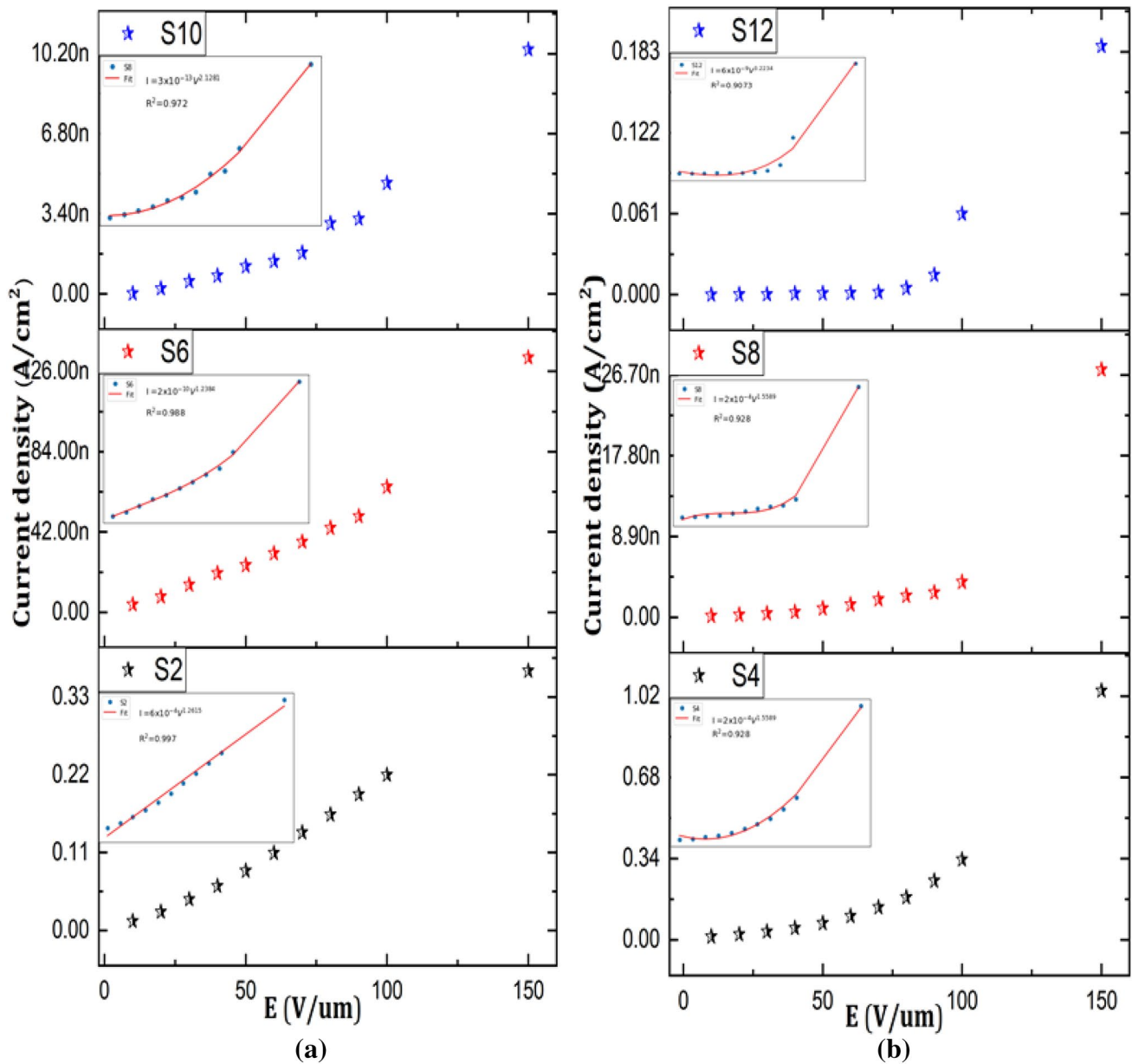


Fig. 7 *J* versus *E* characteristics of films **a** *J* versus *E* characteristics of film in group 2, **b** *J* versus *E* characteristics of films in group 4

Table 3 Electrical resistivity and turn-on field of diamond films grown at different nitrogen concentrations

Group	Sample	N ₂ flow (sccm)	Surface resistivity (Ω cm)	Turn-on Field (V/μm)
2	S2	0	8.0×10^3	–
	S6	2.0	8.1×10^3	–
	S10	20	4.7×10^3	–
4	S4	0	6.4×10^3	30
	S8	4	5.8×10^3	35
	S12	40	3.1×10^3	~72

chamber before deposition, the PL spectra obtained from CVD diamonds can show the presence of neutral or negative nitrogen-vacancy defects. The NV defect translates into PL peaks at 575 and 637 nm, where the 575 and 637 nm peaks correspond to a nitrogen atom bonded to the nearest vacancy and to the vacancy trapped at a substitutional nitrogen atom respectively [48]. The observed nitrogen related peaks are broad. The broadness might be indicative of the presence of other defects in the CVD grown diamonds [48]. In group 2, sample S2 shows a peak at 575.9 nm different from the 575 nm line. This peak is also believed to be associated with nitrogen features in the sample [49]. In an earlier work, Gu

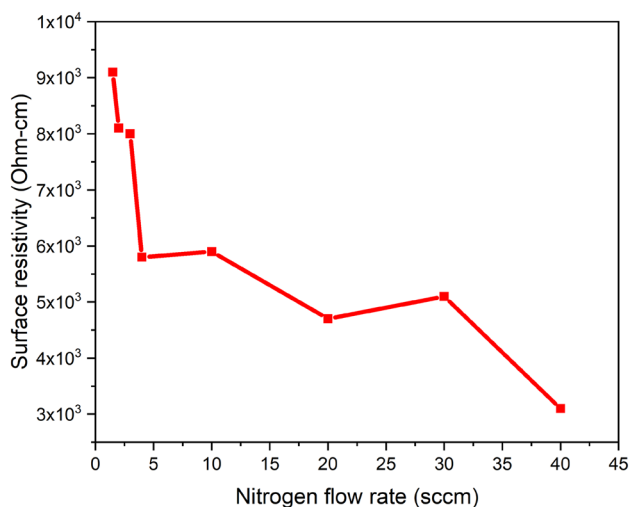


Fig. 8 Electrical resistivity of doped samples as a function of nitrogen flow rates. High nitrogen flow rates in the gas phase mixture leads to a decrease in resistivity

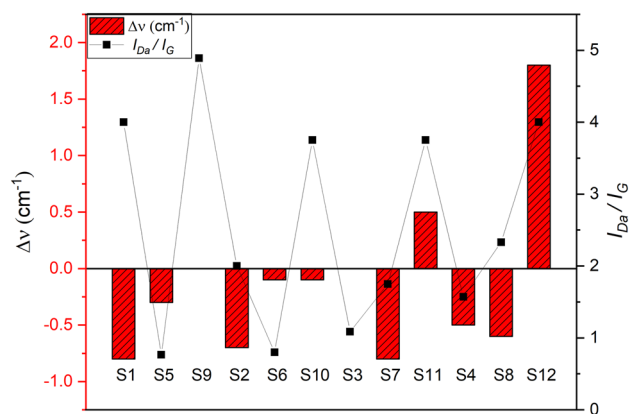


Fig. 9 Graphical representation of shifts in the Raman lines and the ratio of the intensity of diamond peak to amorphous carbon peaks. Positive Raman line shift in sample S12 and S11 results from intrinsic stresses in the films

et al. [49] have shown that the 575.9 nm peak is common in milky type IaB diamonds. The formation of this nitrogen related peak in sample S2 is due to the baseline pressure we operated at before deposition [27].

The relative intensity of NV centres shown in Fig. 4b reveals the formation of predominantly neutral NV centres on the surface of some of the deposited films. This condition as explained by Santori et al. [50] is due to the formation of electronic acceptor layers at the diamond surface. At the surface region, nitrogen donors are ionized thereby making it impossible to donate an electron to the NV centre. A potential acceptor candidate is an amorphous carbon (sp^2) element deposited alongside diamond during the CVD

growth process [51]. In addition, because shallow optical centres are formed at the surface, NV centres at the surface may not be stable [40, 52]. Samples showing the formation of neutral NV centres need further processing to convert the neutral NVs to negatively charged NVs. Surface oxygenation at about 465 °C may be a useful method to induce charge state conversion for the grown diamond films [40, 48, 53].

To understand the influence of microwave power density and pressure on the formation of negatively charged NVs, an additional experiment was done at 6.7 kPa working pressure and 900 W microwave power, while keeping the rest of the parameters for sample S10 in group 2 constant (200 sccm of hydrogen, 1 sccm of methane, 20 sccm of nitrogen, 4 kPa pressure, 800 Watt microwave power). The PL spectra obtained from the experiment is shown in Fig. 10. Contrary to the formation of neutral NV center in sample S10, the spectra of New S10 clearly shows the formation of both neutral and negatively charged NVs. This implies that higher microwave power density and pressure may increase the etching of unwanted carbon phases thereby making it possible to observe the photoluminescence of negative NV centers. It is also possible that at low pressure, nucleation is enhanced and as a result causes electron sinks at grain boundaries [54]. This is another possible explanation for the dominance of neutral NVs in samples grown at 4 kPa pressure.

From the PL spectra obtained in Figs. 3 and 4, it can be concluded that the introduction of high nitrogen (10–40 sccm) concentration in the CVD process will always lead to a formation of neutral NV centers in diamond films. Also, increasing nitrogen concentration from 10–40 sccm results in broader 575 nm peaks. The introduction of a low

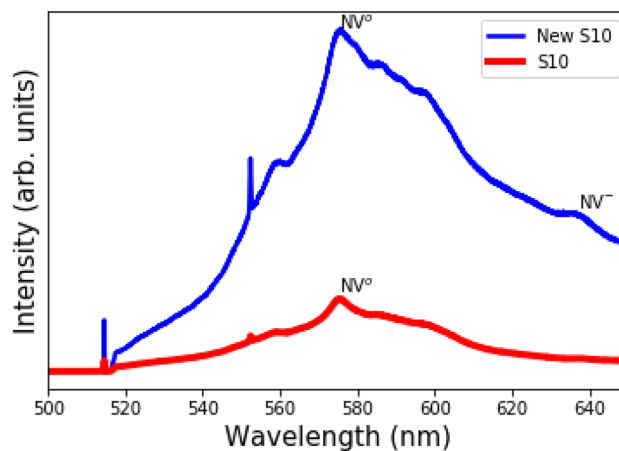


Fig. 10 Comparison between sample New S10 and sample S10. Sample New S10 was deposited with 6.7 kPa pressure, 900 W microwave power while keeping other growth parameters for S10 constant (800 W microwave power, 4 kPa pressure, 200 sccm of hydrogen, 1 sccm of methane, and 20 sccm of nitrogen). Formation of neutral and negative NV is observed in sample New S10

concentration of nitrogen impurities might not yield any surface optical centers. This result is not in agreement with the work of Watanabe et al. [41] where they have reported the formation of negatively charged NV centres while using extremely low nitrogen flow rates. The possible reasons for this disparity might be the difference in growth parameters or the substrate used. Watanabe et al. [41] have shown the formation of negative NV centers homoepitaxially. Demonstrating the presence of NV centers on foreign substrates like silicon is a way to engineer cheap optical centers needed for sensing applications.

The total reflectance of the film modelled by the Fresnel's equation at normal incidence in Ref. [55] depends on several factors. In this case, the surface texture, and density variations due to defects in the materials among other factors appear to account for this variation. The difference in reflectance observed in the deposited films is closely connected with crystal imperfections [56]. Highly doped films with stacking faults, dislocations, and impurities inclusion will show a significant decrease in surface reflectance compared to undoped or minimally doped films. Zuiker et al. [57] showed that the reflectance of thin film diamonds decreases with an increase in CH₄ content. Here, it was observed that the reflectance of the grown films decreases with an increase in nitrogen content. Poor optically detected magnetic resonance (ODMR) contrast are obtained from films with high nitrogen concentration. Films with high concentration of nitrogen impurity (20–40 sccm) are unsuitable for sensing applications due to their poor reflectance properties. Although, sample S9 in group 1 has also been doped with a high nitrogen flow rate (10 sccm), no changes in the intensity of reflectance spectra was observed when compared to its counterparts in group 1, for this reason, sample S9 is suitable for sensing applications.

4.4 Electrical properties of films

The addition of nitrogen impurity in polycrystalline diamond led to a decrease in the surface electrical resistivity of samples as shown in Table 3. This is likely because nitrogen atoms act as a donor in the diamond films and, as a consequence, decreasing the bandgap of diamond. Extensive results showing the same pattern are reported in Refs. [58–62]. As further described by Tsuchiya et al. [63], the decrease in electrical resistivity with medium and high flow rates of nitrogen doping is connected to the formation of sp² C–N bonds on the surface of the deposited films.

The observed decrease in the resistivity of sample S2 in group 2 as compared to doped sample S6 in the same group is associated with transfer doping caused by surface hydrogenation of the sample [63]. It is possible that due to the large volume of hydrogen used during the growth process, hydrogen impurities are present in electrically active

sites which is a reason for the slight decrease in resistivity [64, 65]. In addition, it is possible to further explain the decrease in surface resistivity of samples in terms of I_{Da}/I_G , an increase in the ratio of I_{Da} to I_G results into a decrease in surface resistivity. This implies, the better the diamond quality, the lower the resistivity. In summary, introducing high flow rates of nitrogen in polycrystalline films led to a decrease in the surface electrical resistance for the chosen growth parameters.

5 Conclusion

The influence of surface-introduced nitrogen impurities on the morphology, optical, and electrical properties of polycrystalline diamonds deposited at low pressure have been systematically investigated. The studies have been carried out in three flow regimes: no nitrogen addition (0 sccm), medium nitrogen addition (1–4 sccm), and high nitrogen addition (10–40 sccm). Polycrystalline diamond changes colour depending on the amount of nitrogen impurities added. High nitrogen flow rates in polycrystalline diamonds led to an increase in FWHM of diamond peaks. This feature indicates a depreciation in the crystalline quality of deposited diamonds as revealed by SEM micrographs. Signals from nitrogen related optical centres (predominantly neutral NV centres) were mostly detected in the PL spectra of diamond films doped with medium and high nitrogen flow rates. It was established that high flow rate of nitrogen doping (≥ 20 sccm) will lead to a decrease in the reflectance of polycrystalline diamond. However, one of the samples (S9 in group 1) doped with high flow rate of nitrogen exhibited a reasonable FWHM, and presence of both neutral and negatively charged optical centers. In addition, the sample S9 in group 1 exhibited a good reflectance property as shown from the reflectance spectra. With these combination of properties, sample S9 in group 1 may be a suitable material for sensing applications.

The results obtained are important in identifying optimal parameters for the growth of polycrystalline diamonds suitable for sensing applications. Also, the set of experimental parameters described in this work may be useful as a benchmark for the growth of polycrystalline diamonds with NV centres at low pressure.

Acknowledgements This study was financially supported by an NSERC Discovery Grant to GES and MPB. The authors would like to thank the Canada Foundation for Innovation (CFI) for providing the MPCVD equipment used for the diamond deposition in the Plasma Physics Laboratory (PPL). The first author would like to thank Adeagbo E. Bamise of the Department of Electrical and Computer Engineering for setting up the I–V measurement apparatus.

Funding Funding was provided by Natural Sciences and Engineering Research Council of Canada.

References

- P. Hess, The mechanical properties of various chemical vapor deposition diamond structures compared to the ideal single crystal. *J. Appl. Phys.* **111**(5), 3 (2012)
- J. Field, The mechanical and strength properties of diamond. *Rep. Prog. Phys.* **75**(12), 126505 (2012)
- V. Blank, M. Popov, G. Pivovarov, N. Lvova, S. Terentev, Mechanical properties of different types of diamond. *Diam. Relat. Mater.* **8**(8–9), 1531–1535 (1999)
- A. Erdemir, O. Eryilmaz, G. Fenske, Synthesis of diamondlike carbon films with superlow friction and wear properties. *J. Vac. Sci. Technol.* **18**(4), 1987–1992 (2000)
- S. Cygan, L. Jaworska, P. Putyra, W. Ratuszek, J. Cyboron, P. Klimczyk, Thermal stability and coefficient of friction of the diamond composites with the titanium compound bonding phase. *J. Mater. Eng. Perform.* **26**(6), 2593–2598 (2017)
- D. Meng, W. Yue, F. Lin, C. Wang, Z. Wu, Thermal stability of ultrahard polycrystalline diamond composite materials. *J. Superhard Mater.* **37**(2), 67–72 (2015)
- D. Martínez-Martínez, C. López-Cartés, R. Gago, A. Fernández, J.C. Sánchez-López, Thermal stability and oxidation resistance of nanocomposite tic/a-c protective coatings. *Plasma Process. Polym.* **6**(S1), S462–S467 (2009)
- S.-F. Wang, Y.-F. Hsu, F.-C. Ku, Z.-Y. Liu, The effects of boron dopant on the thermal stability, semiconductor characteristic and wear resistance of diamond films. *Mater. Res. Innov.* **21**(6), 358–366 (2017)
- A. Grill, Electrical and optical properties of diamond-like carbon. *Thin Solid Films* **355**, 189–193 (1999)
- K. Honglertkongsakul, P. May, B. Paosawatyanong, Electrical and optical properties of diamond-like carbon films deposited by pulsed laser ablation. *Diam. Relat. Mater.* **19**(7–9), 999–1002 (2010)
- R.P. Mildren, *Intrinsic optical properties of diamond*, Optical Engineering of Diamond (Wiley, New Jersey, 2013), pp. 1–34
- L. Hounsoume, R. Jones, P. Martineau, M. Shaw, P. Briddon, S. Öberg, A. Blumenau, N. Fujita, Optical properties of vacancy related defects in diamond. *Phys. Status Solidi* **202**(11), 2182–2187 (2005)
- L. Booth, S.A. Catledge, D. Nolen, R.G. Thompson, Y.K. Vohra, Synthesis and characterization of multilayered diamond coatings for biomedical implants. *Materials* **4**(5), 857–868 (2011)
- G. Bogdan, M. Nesládek, J. D’Haen, K. Haenen, M. D’Olielaeager, Freestanding (100) homoepitaxial cvd diamond. *Diam. Relat. Mater.* **15**(4–8), 508–512 (2006)
- C.J. Wort, R.S. Balmer, Diamond as an electronic material. *Mater. Today* **11**(1–2), 22–28 (2008)
- A. Denisenko, E. Kohn, Diamond power devices, concepts and limits. *Diam. Relat. Mater.* **14**(3–7), 491–498 (2005)
- G. Balasubramanian, I. Chan, R. Kolesov, M. Al-Hmoud, J. Tisler, C. Shin, C. Kim, A. Wojcik, P.R. Hemmer, A. Krueger et al., Nanoscale imaging magnetometry with diamond spins under ambient conditions. *Nature* **455**(7213), 648 (2008)
- J. Taylor, P. Cappellaro, L. Childress, L. Jiang, D. Budker, P. Hemmer, A. Yacoby, R. Walsworth, M. Lukin, High-sensitivity diamond magnetometer with nanoscale resolution. *Nat. Phys.* **4**(10), 810 (2008)
- M.W. Doherty, N.B. Manson, P. Delaney, F. Jelezko, J. Wrachtrup, L.C. Hollenberg, The nitrogen-vacancy colour centre in diamond. *Phys. Rep.* **528**(1), 1–45 (2013)
- F. Jelezko, J. Wrachtrup, Single defect centres in diamond: a review. *Phys. Status Solidi* **203**(13), 3207–3225 (2006)
- G. Kucsko, P. Maurer, N.Y. Yao, M. Kubo, H. Noh, P. Lo, H. Park, M.D. Lukin, Nanometre-scale thermometry in a living cell. *Nature* **500**(7460), 54 (2013)
- E. Abe, K. Sasaki, Tutorial: magnetic resonance with nitrogen-vacancy centers in diamond-microwave engineering, materials science, and magnetometry. *J. Appl. Phys.* **123**(16), 161101 (2018)
- R. John, J. Lehnert, M. Mensing, D. Spemann, S. Pezzagna, J. Meijer, Bright optical centre in diamond with narrow, highly polarised and nearly phonon-free fluorescence at room temperature. *N. J. Phys.* **19**(5), 053008 (2017)
- I. Lovchinsky, J. Sanchez-Yamagishi, E. Urbach, S. Choi, S. Fang, T. Andersen, K. Watanabe, T. Taniguchi, A. Bylinskii, E. Kaxiras et al., Magnetic resonance spectroscopy of an atomically thin material using a single-spin qubit. *Science* **355**, 503–507 (2017)
- C. Descamps, D. Tromson, M. Guerrero, C. Mer, E. Rzepka, M. Nesládek, P. Bergonzo, Nitrogen-doped diamond: Thermoluminescence and dosimetric applications. *Diam. Relat. Mater.* **15**(4–8), 833–837 (2006)
- M. Lobaev, A. Gorbachev, S. Bogdanov, A. Vikharev, D. Radishev, V. Isaev, V. Chernov, M. Drozdov, Influence of cvd diamond growth conditions on nitrogen incorporation. *Diam. Relat. Mater.* **72**, 1–6 (2017)
- C. Yap, K. Ansari, S. Xiao, S. Yee, R. Chukka, D. Misra, Properties of near-colourless lightly boron doped cvd diamond. *Diam. Relat. Mater.* **88**, 118–122 (2018)
- J. Freitas Jr., K. Doverspike, P. Klein, Y. Khong, A. Collins, Luminescence studies of nitrogen-and boron-doped diamond films. *Diam. Relat. Mater.* **3**(4–6), 821–824 (1994)
- B. Yan, X. Jia, C. Fang, N. Chen, Y. Li, S. Sun, H.-A. Ma, The effect of phosphorus and nitrogen co-doped on the synthesis of diamond at high pressure and high temperature. *Int. J. Refract. Metals Hard Mater.* **54**, 309–314 (2016)
- Cvd-based reactors, <https://www.plasmionique.com/cvd-mocvd-horizontal-furnace>
- S. Praver, R.J. Nemanich, Raman spectroscopy of diamond and doped diamond. *Phil. Trans. R. Soc. Lond. A* **362**(1824), 2537–2565 (2004)
- A.C. Ferrari, J. Robertson, Raman spectroscopy of amorphous, nanostructured, diamond-like carbon, and nanodiamond. *Phil. Trans. R. Soc. Lond. A* **362**(1824), 2477–2512 (2004)
- L. Krishnia, P.K. Tyagi, Growth and characterization of polycrystalline diamond films on silicon using sugarcane bagasse as carbon precursor at atmospheric pressure by thermal chemical vapor deposition. *Diam. Relat. Mater.* **87**, 18–26 (2018)
- G. Degutis, P. Pobedinskas, S. Turner, Y.-G. Lu, S. Al Riyami, B. Ruttens, T. Yoshitake, J. D’Haen, K. Haenen, J. Verbeeck et al., Cvd diamond growth from nanodiamond seeds buried under a thin chromium layer. *Diam. Relat. Mater.* **64**, 163–168 (2016)
- K.S. Pal, A.K. Mallik, N. Dandapat, N.R. Ray, S. Datta, S. Bysakh, B.K. Guha, Microscopic properties of mpcvd diamond coatings studied by micro-Raman and micro-photoluminescence spectroscopy. *Bull. Mater. Sci.* **38**(2), 537–549 (2015)
- E. Gheeraert, A. Deneuville, A. Bonnot, L. Abello, Defects and stress analysis of the Raman spectrum of diamond films. *Diam. Relat. Mater.* **1**(5–6), 525–528 (1992)
- L. Cançado, K. Takai, T. Enoki, M. Endo, Y. Kim, H. Mizusaki, A. Jorio, L. Coelho, R. Magalhaes-Paniago, M. Pimenta, General equation for the determination of the crystallite size l_a of nanographite by raman spectroscopy. *Appl. Phys. Lett.* **88**(16), 163106 (2006)
- R.E. Clausing, M. Prelas, G. Popovici, L. Bigelow, *Diamond morphology, Handbook of industrial diamonds and diamond films* (Marcel Dekker, New York, 1997), pp. 19–48

39. H.S. Jung, H.H. Park, S.S. Pang, S.Y. Lee, The correlation between the laser energy density and the properties of diamond-like carbon films with nd: Yag (355 nm) excimer laser. *J. Korean Phys. Soc.* **33**, S423–S426 (1998)
40. R. Schirhagl, K. Chang, M. Loretz, C.L. Degen, Nitrogen-vacancy centers in diamond: nanoscale sensors for physics and biology. *Ann. Rev. Phys. Chem.* **65**, 83–105 (2014)
41. H. Watanabe, H. Umezawa, T. Ishikawa, K. Kaneko, S. Shikata, J. Ishi-Hayase, K.M. Itoh, Formation of nitrogen-vacancy centers in homoepitaxial diamond thin films grown via microwave plasma-assisted chemical vapor deposition. *IEEE Trans. Nanotechnol.* **15**(4), 614–618 (2016)
42. A.M. Wojciechowski, M. Karadas, A. Huck, C. Osterkamp, S. Jankuhn, J. Meijer, F. Jelezko, U.L. Andersen, Contributed review: Camera-limits for wide-field magnetic resonance imaging with a nitrogen-vacancy spin sensor. *Rev. Sci. Instrum.* **89**(3), 031501 (2018)
43. J. Yang, C. Li, F. Lu, G. Chen, W. Tang, Y. Tong, Microstructure and fracture strength of different grades of freestanding diamond films deposited by a dc arc plasma jet process. *Surf. Coat. Technol.* **192**(2–3), 171–176 (2005)
44. J. Yang, X. Duan, F. Lu, C. Li, T. Zuo, F. Wang, The influence of dark feature on optical and thermal property of dc arc plasma jet cvd diamond films. *Diam. Relat. Mater.* **14**(10), 1583–1587 (2005)
45. J. Birrell, J. Carlisle, O. Auciello, D. Gruen, J. Gibson, Morphology and electronic structure in nitrogen-doped ultrananocrystalline diamond. *Appl. Phys. Lett.* **81**(12), 2235–2237 (2002)
46. P. Zapol, M. Sternberg, L.A. Curtiss, T. Frauenheim, D.M. Gruen, Tight-binding molecular-dynamics simulation of impurities in ultrananocrystalline diamond grain boundaries. *Phys. Rev. B* **65**(4), 045403 (2001)
47. K. Ohno, E. Joseph Heremans, L.C. Bassett, B.A. Myers, D.M. Toyli, A.C. Bleszynski Jayich, C.J. Palmstrøm, D.D. Awschalom, Engineering shallow spins in diamond with nitrogen delta-doping. *Appl. Phys. Lett.* **101**, 082413 (2012)
48. J. Narayan, A. Bhaumik, Novel synthesis and properties of pure and nv-doped nanodiamonds and other nanostructures. *Mater. Res. Lett.* **5**(4), 242–250 (2017)
49. T. Gu, W. Wang, Optical defects in milky type iab diamonds. *Diam. Relat. Mater.* **89**, 322–329 (2018)
50. C. Santori, P.E. Barclay, K.-M.C. Fu, R.G. Beausoleil, Vertical distribution of nitrogen-vacancy centers in diamond formed by ion implantation and annealing. *Phys. Rev. B* **79**(12), 125313 (2009)
51. J. Ristein, Electronic properties of diamond surfaces-blessing or curse for devices? *Diam. Relat. Mater.* **9**(3–6), 1129–1137 (2000)
52. M. Hauf, B. Grotz, B. Naydenov, M. Dankerl, S. Pezzagna, J. Meijer, F. Jelezko, J. Wrachtrup, M. Stutzmann, F. Reinhard et al., Chemical control of the charge state of nitrogen-vacancy centers in diamond. *Phys. Rev. B* **83**(8), 081304 (2011)
53. K.-M. Fu, C. Santori, P. Barclay, R. Beausoleil, Conversion of neutral nitrogen-vacancy centers to negatively charged nitrogen-vacancy centers through selective oxidation. *Appl. Phys. Lett.* **96**(12), 121907 (2010)
54. A. Stacey, I. Aharonovich, S. Praver, J.E. Butler, Controlled synthesis of high quality micro/nano-diamonds by microwave plasma chemical vapor deposition. *Diam. Relat. Mater.* **18**(1), 51–55 (2009)
55. W. Jacob, A.V. Keudell, T. Schwarz-Selinger, Infrared analysis of thin films amorphous, hydrogenated carbon on silicon. *Braz. J. Phys.* **30**(3), 508–516 (2000)
56. Y.V. Shvyd'ko, S. Stoupin, A. Cunsolo, A.H. Said, X. Huang, High-reflectivity high-resolution X-ray crystal optics with diamonds. *Nat. Phys.* **6**(3), 196 (2010)
57. C.D. Zuiker, D.M. Gruen, A.R. Krauss, In situ laser reflectance interferometry measurement of diamond film growth. *J. Appl. Phys.* **79**(7), 3541–3547 (1996)
58. A. Helmbold, D. Meissner, Optical absorption of amorphous hydrogenated carbon thin films. *Thin Solid Films* **283**(1–2), 196–203 (1996)
59. J.O. Welch, P. Li, A. Chaudhary, R. Edgington, R.B. Jackman, The influence of surface functionalisation on the electrical properties and thermal stability of nanodiamonds. *J. Appl. Phys.* **116**(13), 133705 (2014)
60. T. Kondo, I. Neitzel, V.N. Mochalin, J. Urai, M. Yuasa, Y. Gogotsi, Electrical conductivity of thermally hydrogenated nanodiamond powders. *J. Appl. Phys.* **113**(21), 214307 (2013)
61. S.C. Ray, W. Mbiombi, P. Papakonstantinou, Electrical and electronic properties of nitrogen doped amorphous carbon (a-cnx) thin films. *Curr. Appl. Phys.* **14**(12), 1845–1848 (2014)
62. M. Ullah, E. Ahmed, F. Hussain, A.M. Rana, R. Raza, Electrical conductivity enhancement by boron-doping in diamond using first principle calculations. *Appl. Surf. Sci.* **334**, 40–44 (2015)
63. M. Tsuchiya, K. Murakami, K. Magara, K. Nakamura, H. Ohashi, K. Tokuda, T. Takami, H. Ogasawara, Y. Enta, Y. Suzuki et al., Structural and electrical properties and current–voltage characteristics of nitrogen-doped diamond-like carbon films on si substrates by plasma-enhanced chemical vapor deposition. *Jpn. J. Appl. Phys.* **55**(6), 065502 (2016)
64. F. Zhang, W. Zhang, M. Chen, G. Chen, X. Jiang, Study on I–V characteristics of diamond films synthesized by dc arc discharge plasma chemical vapour deposition. *Thin Solid Films* **205**(1), 39–42 (1991)
65. M. Landstrass, K.V. Ravi, Resistivity of chemical vapor deposited diamond films. *Appl. Phys. Lett.* **55**(10), 975–977 (1989)

Publisher's Note Springer Nature remains neutral with regard to jurisdictional claims in published maps and institutional affiliations.